

Quasi-degeneracies in a 2-spin system: symmetry aspects and a perturbational approach to tunnel splitting

L. Schatzer, W. Breyermann, H. Thomas

Institut für Physik der Universität Basel, Klingelbergstrasse 82, CH-4056 Basel, Switzerland

Received: 17 July 1995 / Revised version: 11 December 1995

Abstract. A large number of energy levels in different invariant subspaces of the anisotropic XY -model are quasi-degenerate in a wide parameter range, i.e., their spacing is much smaller than the mean level spacing of the system. These quasi-degeneracies can be interpreted in two ways: (i) as tunnel splitting, (ii) as weak level splitting related to a parametric point of exact degeneracy. Starting from the second interpretation we calculate the tunnel splitting by use of perturbative methods.

PACS: 75.10.Jm; 3.65.-w

1. Introduction

The subject of this paper is to study the quasi-splitting of the energy levels for a spin system. Our results are of interest in the context of spin tunneling; they provide a simple method for calculating the tunnel splitting for this system.

Spin tunneling has raised growing interest during the last years. It turned out to be important, e.g., in nucleation phenomena (e.g., bubbles in ferromagnets [1, 2] and antiferromagnets [3]) and in macroscopic quantum effects occurring in the quantum dynamics of large domain-walls pinned at defects [4]. The latter is also of practical interest because it imposes limits on the lifetime of information storage on magnetic devices [5, 6].

Tunnel splitting is typically evaluated by semi-classical methods such as the WKB method or the instanton technique in the framework of the path integral formalism. Semi-classical methods for spin systems have been developed during the last years. Enz and Schilling [7] calculated the tunnel splitting using the instanton method, and Hemmen and Sütö [8] did the same calculation by a generalization of the conventional WKB method. In both cases, the system consists of a single spin submitted to an anisotropic crystal field and a magnetic field; it is described by the Hamiltonian

$$H = -A\hat{S}_x^2 + B\hat{S}_z^2 - h\hat{S}_x. \quad (1)$$

By both methods one finds for $h = 0$ in the semi-classical limit a tunnel splitting of the form [7]

$$\Delta E = 16A\hbar^2 s^{3/2} (1+b)^{3/4} \left(\frac{b^{1/2}}{1+(1+b)^{1/2}} \right)^{2s+1}, \quad (2)$$

where $b = B/A$, and s is the spin quantum number. As usual for spin tunneling, the strength of the level splitting vanishes algebraically with the field strength h . The dependence on the spin length s is exponential.

Reviews of the path-integral approach and the WKB method for spin systems are given in [9] and [10], respectively. Almost all applications are restricted to the case of a single spin; only recently the WKB method has been applied to a pair of antiferromagnetically coupled spins [10]. The path-integral approach, on the other hand, demands a vast analytical effort already in the one-spin case. In this situation, alternative methods would be of great help. If tunneling could be associated with symmetry breaking, perturbation theory would be a good candidate. In the case of potential systems, however, tunnel splitting cannot be calculated by perturbation theory. Indeed, for the standard example of a symmetric double-well potential the splitting of the ground state is proportional to $\hbar \exp\{-C/\hbar\}$, the constant C being approximately proportional to the height of the barrier [11]. If one considers the case of an infinite potential barrier as unperturbed system, any transition to a perturbed system with *finite* barrier results in a singular perturbation. As a consequence, tunnel splitting and splitting caused by symmetry breaking are different phenomena which must be dealt with by different techniques.

Recently, however, Garanin pointed out [12] that in the case of (1) tunnel splitting can actually be calculated by means of standard perturbation theory in an elementary way; this was also recognized by Weigert [13]. The same fact is at the basis of the WKB approach presented in [10]. In addition, the perturbational method allows one to evaluate the splitting not only for the ground states but for *all* levels, and the result is valid not only in the semiclassical limit but for arbitrary spin lengths.

The perturbational approach is possible because tunnel splitting vanishes precisely for those parameter values ($h = 0$ and $B = 0$) for which the system has an additional C_∞ symmetry. Thus, tunnel splitting, which is present for $h \neq 0$ or $B \neq 0$, can equally well be interpreted as splitting caused by symmetry breaking and calculated by the techniques of

degenerate perturbation theory. The latter is conceptually well understood and the calculations are straightforward.

We expect the relation between spin tunnel splitting and symmetry breaking to be more than a mere coincidence and to exist more generally. If this hypothesis turns out to be true, it may open the way for dealing with tunneling in many-spin systems. As a first attempt in this direction, we have investigated a system composed of two spins, which can be considered as a generalization of (1).

For a single spin, perturbation theory could be applied directly without appealing for symmetry (as Garanin did), because (i) the unperturbed system (i.e. without tunneling) is given immediately and (ii) the perturbation matrix is very simple. In general, however, an explicit treatment of symmetry is crucial. Accordingly, the proper analysis of the symmetry properties and its consequences on perturbation theory are a central part of this paper. We present it for the 2-spin system introduced in the following section.

The perturbational approach determines our exposition which, from the point of view of tunnel splitting, could appear as putting the cart before the horse. Analyzing the energy spectrum under the hypothesis that tunnel splitting can always be interpreted as symmetry breaking, we start with a phenomenological search for small level splitting (Sect. 3) including the definition of quasi-degeneracy between *different* invariant subspaces of the total Hilbert space. By the use of group theoretical methods, the quasi-degeneracies will be classified according to the symmetry properties of the corresponding subspaces. This yields also the parameter values at which exact degeneracies of the energy eigenvalues and the related (continuous) symmetries occur. After these unevitable preliminaries we present a scheme for numerically evaluating the level splitting by degenerate perturbation theory (Sect. 4). To this end, we use a graphical representation of the perturbation matrix elements inspired by Feynman graphs. This allows us to explicitly calculate the splitting *order* of all level pairs and, to lowest order, the splitting *amplitude* of the ground levels of the XY-model with pure exchange anisotropy. The connection with tunneling is deferred to the discussion (Sect. 5). We conclude with some remarks on the generality of our approach and possible extensions to larger systems.

2. The anisotropic XY-model

We consider the anisotropic two-spin system described by the Hamiltonian

$$\hat{H}_{\alpha\gamma} = -J \left[(1 + \gamma) \hat{S}_1^x \hat{S}_2^x + (1 - \gamma) \hat{S}_1^y \hat{S}_2^y + \frac{1}{2} \alpha \left((\hat{S}_1^x)^2 - (\hat{S}_1^y)^2 + (\hat{S}_2^x)^2 - (\hat{S}_2^y)^2 \right) \right], \quad (3)$$

which has been introduced by Magyari et al. [14]. The parameter J is the coupling strength and α and γ determine the anisotropy of the (one-site) crystal field and the exchange interaction, respectively. The spin operators \hat{S}_i^k satisfy the usual spin commutation relations:

$$\left[\hat{S}_i^k, \hat{S}_j^l \right] = i \hbar \delta_{ij} \sum_{\gamma} \varepsilon_{klm} \hat{S}_i^m \quad (4)$$

Table 1. Character table for the group $D_2 \otimes S_2$

I	E	C_2^z	C_2^y	C_2^x	P	PC_2^z	PC_2^y	PC_2^x
A_{1s}	1	1	1	1	1	1	1	1
A_{1a}	1	1	1	1	-1	-1	-1	-1
B_{1s}	1	1	-1	-1	1	1	-1	-1
B_{1a}	1	1	-1	-1	-1	-1	1	1
B_{2s}	1	-1	1	-1	1	-1	1	-1
B_{2a}	1	-1	1	-1	-1	1	-1	1
B_{3s}	1	-1	-1	1	1	-1	-1	1
B_{3a}	1	-1	-1	1	-1	1	1	-1

In the following, we confine ourselves to the case of spins of the same length, $s_1 = s_2 = s$, which has been studied extensively in [15–17]. Thus, the total Hilbert space of dimension $(2s + 1)^2$ is the direct product $\mathcal{H}^s \otimes \mathcal{H}^s$ of two identical one-spin spaces. The spin quantum number s (indicated as superscript) can be integer or half-integer. Both cases can be treated along the same lines, but one has to account for the different representations of the symmetry group (see below). In order to avoid this complication, which gives no fruitful contribution to our argumentation, the discussion is restricted to half-integer values of s .

The Hamiltonian (3) is invariant under rotations of an angle π around the x -, y -, and z -axes and under the permutation $1 \leftrightarrow 2$ of the spins. Thus, the symmetry group $G = D_2 \otimes S_2$ is the direct product of the point group $D_2 = \{E, C_2^x, C_2^y, C_2^z\}$ and the group $S_2 = \{E, P\}$. Since G is abelian and $|G| = 8$ there are eight one-dimensional irreducible representations (Table 1). Thus the Hilbert space decomposes into eight independent subspaces \mathcal{H}_I which transform corresponding to the representations of G (Table 2)¹. To construct a symmetry-adapted basis, it is convenient to start from the product basis

$$|m_1 m_2\rangle = |s m_1\rangle \otimes |s m_2\rangle, \quad (5)$$

where $|s m\rangle \equiv |s m\rangle_x$ denotes the eigenstates of \hat{S}^x (and *not* those of \hat{S}^z !). The action of the symmetry operations on this basis can be deduced easily from Wigner's D -matrices (cf., e.g. [18, pp. 221–223]) as

$$\begin{aligned} P |m_1 m_2\rangle &= |m_2 m_1\rangle, \\ C_2^x |m_1 m_2\rangle &= (-1)^{m_1+m_2} |m_1 m_2\rangle, \\ C_2^y |m_1 m_2\rangle &= (-1)^{2s} | -m_1 -m_2\rangle, \\ C_2^z |m_1 m_2\rangle &= (-1)^{2s-m_1-m_2} | -m_1 -m_2\rangle. \end{aligned} \quad (6)$$

The symmetry-adapted basis obtained by symmetrization of the states $|m_1 m_2\rangle$ has the form

$$|m_1 m_2 \sigma_1 \sigma_2\rangle = \mathcal{N} \left(|m_1 m_2\rangle + \sigma_1 | -m_1 -m_2\rangle + \sigma_2 |m_2 m_1\rangle + \sigma_1 \sigma_2 | -m_2 -m_1\rangle \right). \quad (7)$$

Here, the σ_i take the values ± 1 and \mathcal{N} is a normalization factor. For a unique representation of the symmetry-adapted

¹ In addition to the elements of G , the Hamiltonian (2) is invariant under time reversal T . Formally this operator reads $\hat{T} = \hat{K} \exp(-i\pi \hat{S}^y)$, where \hat{K} is antilinear and transforms a state $|\Phi\rangle$ into its complex conjugate. Since all representations of the group G are real, $|\Phi\rangle$ and $|\Phi^*\rangle$ are in equivalent representations and T acts essentially as C_2^y . Thus, time-reversal symmetry need not to be explicitly taken into account for the considerations exposed in the following

Table 2. Basis of the invariant subspaces $\mathcal{H}_I \subseteq \mathcal{H}$ for the symmetry $D_2 \otimes S_2$ and half-integer s . The subspaces are labeled by their irreducible representations (left column), which are uniquely determined by the parity of $m_1 + m_2$ and the signs σ_1, σ_2 (of (7) and (8)). The states are written in the \hat{S}^x -representation, m_1 lies in the range $\frac{1}{2} \leq m_1 \leq s$. m_1 and m_2 are both half-integer. The subspace dimensions take only two different values, namely $d_1 = (2s - 1)(2s + 1)/8$ and $d_2 = (2s + 3)(2s - 1)$

I	$ n, I\rangle$	$m_1 + m_2$	m_2 -range	$\dim \mathcal{H}_I$
A_{1s}	$ m_1 m_2 - +\rangle$	even	$-m_1 < m_2 < m_1$	d_1
A_{1a}	$ m_1 m_2 - -\rangle$	even	$-m_1 \leq m_2 < m_1$	d_2
B_{1s}	$ m_1 m_2 - +\rangle$	odd	$-m_1 < m_2 \leq m_1$	d_2
B_{1a}	$ m_1 m_2 - -\rangle$	odd	$-m_1 < m_2 < m_1$	d_1
B_{2s}	$ m_1 m_2 + +\rangle$	odd	$-m_1 < m_2 \leq m_1$	d_2
B_{2a}	$ m_1 m_2 + -\rangle$	odd	$-m_1 < m_2 < m_1$	d_1
B_{3s}	$ m_1 m_2 + +\rangle$	even	$-m_1 \leq m_2 < m_1$	d_2
B_{3a}	$ m_1 m_2 + -\rangle$	even	$-m_1 < m_2 < m_1$	d_1

states (7) one has to restrict the quantum numbers to $m_1 > 0$ and $|m_2| \leq m_1$. The exact range of m_2 depends on the subspace \mathcal{H}_I . In the following the states (7) will be labeled by the short-hand notation

$$|n, I\rangle \equiv |m_1 m_2 \sigma_1 \sigma_2\rangle \quad (8)$$

where $n = (m_1, m_2)$ and I indicates the irreducible representation, which is determined by the parity of $m_1 + m_2$ and the values of the σ_i . For half-integer values of s , the complete basis of the subspaces I is listed in Table 2.

3. Nearest level spacings and quasi-degeneracies

In a single subspace, the distribution $P(\Delta E)$ of nearest level spacings ΔE typically follows Poisson or Wigner statistics depending on whether the classical system is completely integrable or completely chaotic [19]. For the present system, this has been confirmed qualitatively by Srivastava et al. [17]. In the following, a different quantity is studied, namely, the nearest-level spacing of levels contained in *different* subspaces. We define this quantity as

$$\Delta E_n^{(I, I')} = \min_{n'} |E_n^I - E_{n'}^{I'}|. \quad (9)$$

Here, E_n^I ($E_{n'}^{I'}$) denotes the n th (n' th) energy level of the invariant subspace \mathcal{H}_I ($\mathcal{H}_{I'}$). (Notice that, generically, different subspaces are not isomorphic and especially may have different dimensions. Consequently, the nearest-level spacings are not commutative in the indices I and I' , i.e., $\Delta E_n^{(I, I')} \neq \Delta E_{n'}^{(I', I)}$.)

Generically, energy eigenstates of different invariant subspaces are not correlated with each other. Thus, degeneracies of energy levels of different subspaces are expected to occur only accidentally, and so are *quasi*-degeneracies expected to do. The surprising result for the present system is that there are numerous quasi-degeneracies which are not accidental and seemingly not randomly distributed. Typical features of the nearest level spacings are depicted in Figs. 1 and 2 where, for selected pairs of subspaces, the level-spacing distributions are represented as clouds in an $(E_n^I, \Delta E_n^{(I, I')})$ -diagram. Figure 1 shows the plots for the case $(\alpha, \gamma) = (0, 0.5)$ and the subspace combinations $(I, I') = (A_{1s}, A_{1a})$ and (A_{1s}, B_{3s}) , whereas Fig. 2 displays

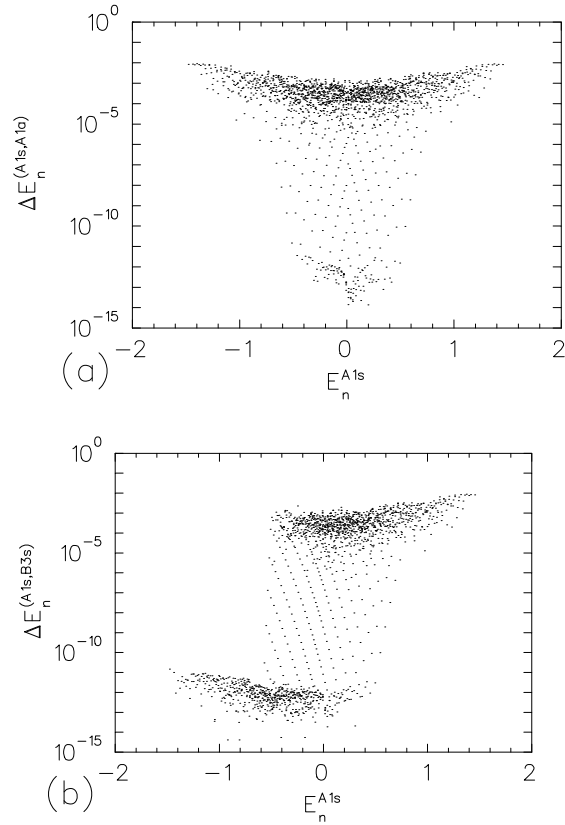


Fig. 1a,b. Nearest level spacings $\Delta E_n^{(I, I')}$ for the system $(\alpha, \gamma) = (0, 0.5)$, $s = 121/2$: **a** $(I, I') = (A_{1s}, A_{1a})$ (class M_1), **b** $(I, I') = (A_{1s}, B_{3s})$ (class M_6). (The classes refer to Table 3.) The number of level pairs is in both cases $n = 1830$. The energies are expressed in reduced units of $J\hbar^2 s^2$. For uncorrelated states one would expect the $\Delta E_n^{(I, I')}$'s to be distributed around the mean level spacing $\Delta E \approx 3 \cdot 10^{-4}$ with only a few quasi-degeneracies due accidental level crossings. There is, however, a surprisingly large number of such points, which, moreover, form an intriguing structure. Note that around $\Delta E_n^{(I, I')} \approx 10^{-12}$ the numerical precision of the routine for determining the eigenvalues is reached

the distribution corresponding to the case $(\alpha, \gamma) = (0.5, 0)$ and the subspace pair $(I, I') = (A_{1s}, B_{2a})$. The spin length is $s = \frac{121}{2}$ in both cases. For uncorrelated subspaces \mathcal{H}_I and $\mathcal{H}_{I'}$ we would expect distributions in the form of featureless clouds centered at the mean level spacing ΔE . The distributions displayed in Figs. 1 and 2, however, exhibit some remarkable structure. Especially, they present two density maxima: one, as expected, at the value of the mean level spacing ΔE , and a second one at a value of the order of 10^{-12} , i.e., of the numerical precision of double precision arithmetics. In addition, one observes a characteristic dependence of the spacings $\Delta E_n^{(I, I')}$ on the levels E_n^I , which is different in each figure.

For the investigation of all subspace combinations (I, I') it turns out to be useful to classify them in the following way. The 28 combinations can be grouped into 7 classes M_i ($i = 1, \dots, 7$) determined by the four-element subgroup $G_i \subset G$ for which both subspaces \mathcal{H}_I and $\mathcal{H}_{I'}$ transform according to the same representation (cf. Table 3). The class M_1 , for instance, is defined by the subgroup $G_1 = D_2$ consisting of the proper rotations. By comparing Tables 1 and 3 one easily recognizes that both subspaces of the pair

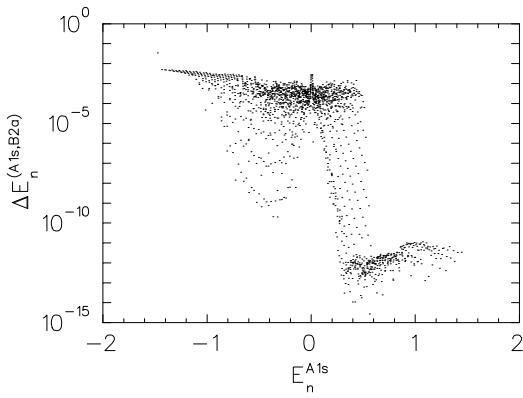


Fig. 2. Nearest level spacings $\Delta E_n^{(A_{1s}, B_{2a})}$ (class M_5) for the system $(\alpha, \gamma) = (0.5, 0)$, $s = 121/2$. The same remarks apply as for Fig. 1

Table 3. Classification of invariant subspace combinations (I, I') . Both subspaces of a pair recorded in the i -th row (right column) transform according to the same irreducible representation of the group G_i (middle column)

Class M_i	Subgroup G_i	(I, I')	
M_1	$\{E, C_2^x, C_2^y, C_2^z\}$	(A_{1s}, A_{1a}) (B_{2s}, B_{2a})	(B_{1s}, B_{1a}) (B_{3s}, B_{3a})
M_2	$\{E, P, C_2^z, PC_2^z\}$	(A_{1s}, B_{1s}) (B_{2s}, B_{3s})	(A_{1a}, B_{1a}) (B_{2a}, B_{3a})
M_3	$\{E, C_2^z, PC_2^x, PC_2^y\}$	(A_{1s}, B_{1a}) (B_{2s}, B_{3a})	(A_{1a}, B_{1s}) (B_{2a}, B_{3s})
M_4	$\{E, P, C_2^y, PC_2^y\}$	(A_{1s}, B_{2s}) (B_{1s}, B_{3s})	(A_{1a}, B_{2a}) (B_{1a}, B_{3a})
M_5	$\{E, C_2^y, PC_2^x, PC_2^z\}$	(A_{1s}, B_{2a}) (B_{1s}, B_{3a})	(A_{1a}, B_{2s}) (B_{1a}, B_{3s})
M_6	$\{E, P, C_2^x, PC_2^x\}$	(A_{1s}, B_{3s}) (B_{1s}, B_{2s})	(A_{1a}, B_{3a}) (B_{1a}, B_{2a})
M_7	$\{E, C_2^x, PC_2^y, PC_2^z\}$	(A_{1s}, B_{3a}) (B_{1s}, B_{2a})	(A_{1a}, B_{3s}) (B_{1a}, B_{2s})

(A_{1s}, A_{1a}) transform according to the identity representation of G_1 , and those of the pair (B_{1s}, B_{1a}) transform according to the representation B_1 of the same subgroup.

We have checked explicitly that for the values of the parameters α and γ in Figs. 1 and 2, subspace pairs of the same class M_i display similar $\Delta E_n^{(I, I')}$ -plots. Enhanced quasi-degeneracies occur in the classes M_1, M_2, M_6 , and M_7 when $(\alpha, \gamma) = (0, 0.5)$. In the case $(\alpha, \gamma) = (0.5, 0)$ the quasi-degeneracies have been observed for the classes M_2, M_3, M_5 , and M_6 .

Actually, exact degeneracies appear for some special parameter values, for which the system has higher symmetry (cf. Table 4). In the following, we will analyze in more detail the quasi-degeneracies occurring for systems located on the $(\alpha = 0)$ -line in parameter space. This line contains three exceptional points, namely $\gamma = -1, 0$, and 1 , where additional rotational symmetries arise. They cause the states *quasi*-degenerate at $\gamma = \frac{1}{2}$ to become *exactly* degenerate at $\gamma = 0$ or $\gamma = 1$. For the latter case this is illustrated by Fig. 3, where the γ -dependance of the nearest-level spacings for the subspace pair (A_{1s}, A_{1a}) is plotted for a system with spin length $s = 9/2$.

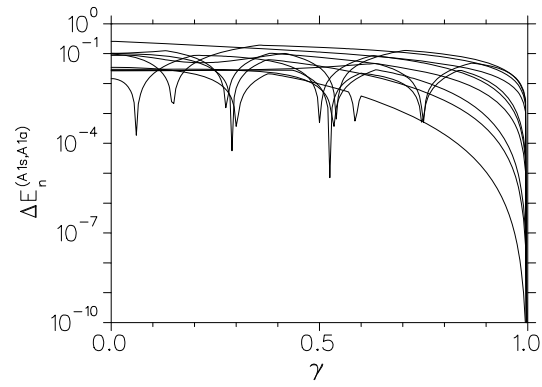


Fig. 3. Nearest level spacings $\Delta E_n^{(A_{1s}, A_{1a})}$ (class M_1) for the system $\alpha = 0$ ($s = 9/2$, 10 level pairs), showing that the quasi degeneracies are related to the exact degeneracies at $\gamma = 1$. The randomly distributed dips occurring for $\gamma \gg 0.4$ indicate the occurrence of accidental degeneracies

Table 4. XY-models with k -fold degeneracies caused by additional symmetries. The notation C_∞^μ indicates full rotational symmetry around the μ -axis, and the argument (i) indicates that spin i may be rotated separately. For $(\alpha, \gamma) = (0, 1)$, e.g., the total symmetry group is given by $G^* = C_\infty^x(1) \otimes C_\infty^x(2) \otimes D_2 \otimes S_2$. The discrete symmetry T^μ (4th and 5th row) is represented by the operator $\hat{T}^\mu = \hat{p}^{(\hat{S}_1^\mu + \hat{S}_2^\mu)/h+1} e^{i\pi(\hat{S}_1^\mu/h+1/2)}$. This operator has no classical analogon

(α, γ)	Additional symmetries	M_i with degeneracies	k
$(0, 0)$	C_∞^z	M_2	2
$(0, 1)$	$C_\infty^x(1), C_\infty^x(2)$	M_1, M_6, M_7	2 and 4
$(0, -1)$	$C_\infty^y(1), C_\infty^y(2)$	M_1, M_4, M_5	2 and 4
$(\neq 0, 1)$	T^x	M_6 or M_7	2
$(\neq 0, -1)$	T^y	M_4 or M_6	2

4. Perturbative approach

4.1. Degenerate perturbation theory for the XY-model with pure exchange anisotropy

The perturbative approach is presented in detail for quasi-degeneracies occurring for $\alpha = 0$ and positive values of γ , which are caused by exact degeneracies at $\alpha = 0$ and $\gamma = 1$. In order to get an unperturbed Hamiltonian

$$\hat{H}_0 = -J\hat{S}_1^x\hat{S}_2^x \quad (10)$$

independent of γ , the Hamiltonian (3) has to be rescaled by $(1 + \gamma)^{-1}$. The eigenstates of \hat{H}_0 are the product states $|m_1 m_2\rangle$ with eigenvalues $-J\hbar^2 m_1 m_2$. Thus, for given values of m_1 and m_2 the symmetrized states $|n, I\rangle \equiv |(m_1 m_2), I\rangle$ are degenerate eigenstates of the unperturbed Hamiltonian. The additional degeneracies are due to invariance of the unperturbed Hamiltonian not only under G but also under a larger group $G^* \supset G$ containing, in addition, arbitrary rotations of the individual spins around their x -axes (Table 4). This larger group has irreducible representations of dimensions two and four: the states $|n, I\rangle$ are contained in four-dimensional representations if $m_1 \neq m_2$ and in two-dimensional representations if $m_1 = m_2 \neq 0$. The total Hamiltonian reads

$$\hat{H}(\lambda) = \hat{H}_0 + \lambda\hat{V}, \quad (11)$$

with the perturbative matrix

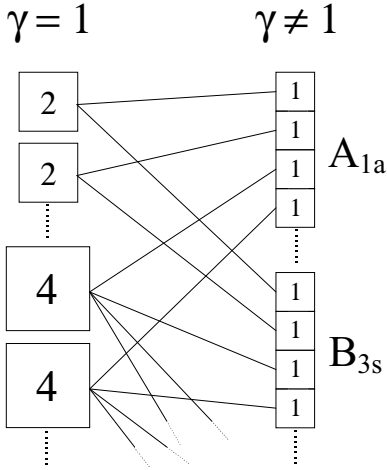


Fig. 4. Relation between the invariant subspaces of \mathcal{H} with respect to the groups G^* (for $\gamma = 1$) and the subspaces \mathcal{H}_I with respect to G (for $\gamma \neq 1$). The 2- and 4-dimensional irreducible representations of G^* split up into 1d irreducible representations of G . From the latter, the equivalent representations span the subspaces \mathcal{H}_I (touching blocks)

$$\hat{V} = -J\hat{S}_1^y\hat{S}_2^y. \quad (12)$$

The perturbation parameter λ is related to the system parameter γ by $\lambda = (1 - \gamma)/(1 + \gamma)$. When $\lambda \neq 0$ ($\gamma \neq 1$), the multidimensional irreducible representations of G^* split into different irreducible one-dimensional representations of G (Fig. 4). Accordingly, states $|n, I\rangle$ with the same values of n and different I happen to belong to different subspaces. These states will be called *correlated*. The corresponding pairs of *correlated subspaces* (I, I') form the already introduced classes M_i ($i = 1, \dots, 7$).

Following standard perturbation theory, the perturbed energy eigenvalues $E_n(\lambda)$ of the Hamiltonian (11) are expanded in a power series:

$$E_n(\lambda) = \varepsilon_n^{(0)} + \lambda\varepsilon_n^{(1)} + \lambda^2\varepsilon_n^{(2)} + \dots, \quad (13)$$

where the coefficients $\varepsilon_n^{(0)}$ give the unperturbed eigenvalues. In the non-degenerate case, the ν th order coefficients $\varepsilon_n^{(\nu)}$ can be expressed as a weighted sum over all non-vanishing cyclic products of ν transition amplitudes V_{ij} :

$$\varepsilon_n^{(\nu)} = \sum_{k_1, \dots, k_{\nu-1}} g_{nk_1 \dots k_{\nu-1}} V_{nk_1} V_{k_1 k_2} \dots V_{k_{\nu-1} n}, \quad (14)$$

where $g_{nk_1 \dots k_{\nu-1}}$ are the usual weight factors. In the representation of the symmetrized basis the matrix V is blockwise diagonal, each block corresponding to an invariant subspace \mathcal{H}_I . Thus, the matrix elements can be written in the form

$$\begin{aligned} \langle (m'_1, m'_2), I' | \hat{V} | (m_1, m_2), I \rangle = & \\ & \left[A \delta_{m'_1, m_1+1} \delta_{m'_2, m_2+1} + B \delta_{m'_1, m_1+1} \delta_{m'_2, m_2-1} \right. \\ & + C \delta_{m'_1, m_1-1} \delta_{m'_2, m_2+1} + D \delta_{m'_1, m_1-1} \delta_{m'_2, m_2-1} \\ & \left. + E \delta_{m'_1, m_1} \delta_{m'_2, m_2} \right] \delta_{II'}. \end{aligned} \quad (15)$$

In general, the factors A, B, C, D and E , which are given explicitly in Appendix 5, depend on $n = (m_1, m_2)$ and I . We emphasize, however, that they do *not* depend on I , when

$|m_2| < m_1 - 2$. Consequently, the corresponding matrix elements are identical, which is one of two essential ingredients for the occurrence of quasi-degeneracies.

Since the perturbative matrix is block-diagonal, each block corresponding to one subspace \mathcal{H}_I , the equations for the perturbed energy levels can be written down separately for each subspace \mathcal{H}_I . The restricted Hamiltonians $\hat{H}^I(\lambda) = \hat{H}_0^I + \lambda\hat{V}^I$ are obtained easily from (11–12) by projections onto the different subspaces. Accordingly, the perturbed energy eigenvalues for two subspaces \mathcal{H}_I and $\mathcal{H}_{I'}$ read

$$E_n^I(\lambda) = \varepsilon_n^{I,(0)} + \lambda\varepsilon_n^{I,(1)} + \lambda^2\varepsilon_n^{I,(2)} + \dots \quad (16)$$

$$E_n^{I'}(\lambda) = \varepsilon_n^{I',(0)} + \lambda\varepsilon_n^{I',(1)} + \lambda^2\varepsilon_n^{I',(2)} + \dots, \quad (17)$$

where the terms $\varepsilon_n^{I,(\nu)}$ and $\varepsilon_n^{I',(\nu)}$ are both of the form of (14). We are interested in comparing the influence of the perturbation on the energy level of a state $|n, I\rangle$ to its influence on the level of the correlated state $|n, I'\rangle$. In the following we assume that a state $|n, I\rangle$ is not degenerate in the subspace \mathcal{H}_I itself. However, *several* states $|n, I'\rangle, |n, I''\rangle$ contained in *different* subspaces $\mathcal{H}_{I'}, \mathcal{H}_{I''}$ may be correlated to them. Up to lowest order in λ the energy difference of correlated states

$$\Delta E_n^{(I, I')}(\lambda) = \left| E_n^I(\lambda) - E_n^{I'}(\lambda) \right| \quad (18)$$

is given by

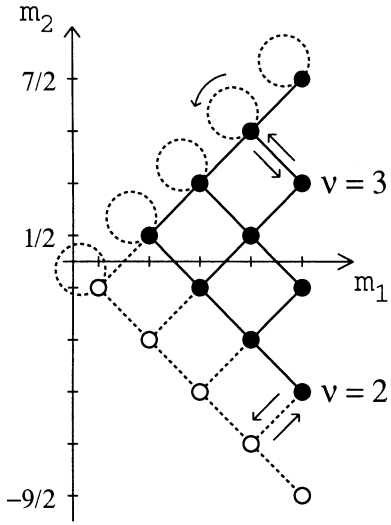
$$\Delta E_n^{(I, I')}(\lambda) = \eta_n \lambda^{\nu_n} + o(\lambda^{\nu_n}) \quad (19)$$

where $\eta_n = |\varepsilon_n^{I,(\nu_n)} - \varepsilon_n^{I',(\nu_n)}|$ is the first non-vanishing difference of the corresponding expansion coefficients, and $\nu_n = \nu_n^{(I, I')}$ is the splitting order. The latter depends on the pair $(|n, I\rangle, |n, I'\rangle)$ of correlated states. To evaluate the actual value of ν_n , one has to compare the perturbation series (16) and (17), and look for the lowest-order term that is different in these expansions. This is equivalent to looking for the lowest order at which one of the following conditions is met: either a pair of non-identical cyclic products $V_{nk_1}^I \dots V_{k_{\nu-1}n}^I \neq V_{nk_1}^{I'} \dots V_{k_{\nu-1}n}^{I'}$ or a product $V_{nk_1}^I \dots V_{k_{\nu-1}n}^I$ contains an uncorrelated state. Note that the weight factors $g_{nk_1 \dots k_{\nu-1}}$, which only depend on the properties of the *unperturbed* system, do not enter the discussion. Indeed, assuming the usual form [18, p.285ff]

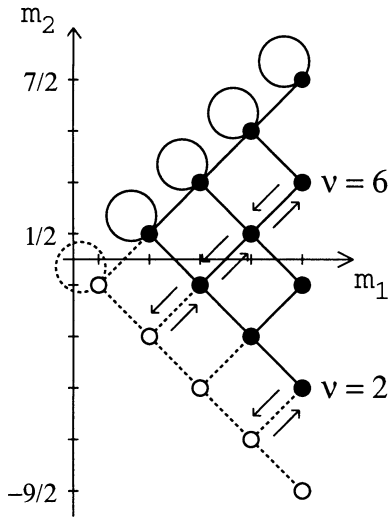
$$g_{nk_1 \dots k_l}^I = \prod_{k_i} (E_n^I(0) - E_{k_i}^I(0))^{-1} \quad \text{if } k_i \neq n, \quad (20)$$

$g_{nk_1 \dots k_l}^I$ and $g_{nk_1 \dots k_l}^{I'}$ are identical if the unperturbed energies are degenerate.

We introduce a graphical method for comparing the perturbation matrices of correlated subspaces. First note that the states $|m_1, m_2\rangle$ can be represented as points regularly arranged on a square lattice of side length $2s$, which is centered at the origin of the (m_1, m_2) plane. Accordingly, the states $|m_1, m_2, I\rangle$ of the subspace \mathcal{H}_I will be represented as points on a sublattice located inside a triangle bounded by the diagonals and the right border of the square lattice. In this picture, the non-zero elements of the submatrix of \hat{V} corresponding to \mathcal{H}_I appear as links between lattice points. Due to the special structure of \hat{V} , which is a sparse



(a)



(b)

Fig. 5a,b. Graphical representation of the Hamiltonian $\hat{H}(\lambda) = -J(\hat{S}_1^x \hat{S}_2^x + \lambda \hat{S}_1^y \hat{S}_2^y)$ in the correlated subspaces (I, I') : **a** $(I, I') = (A_{1s}, A_{1a})$, $\nu_n = m_1 - |m_2|$, **b** $(I, I') = (A_{1s}, B_{3s})$, $\nu_n = m_1 + m_2$. Equivalent and non-equivalent states $|(m_1, m_2), I\rangle$ are represented as points and circles, equivalent and non-equivalent matrix elements as full and dashed lines, respectively. The pair of shortest non-equivalent cyclic products must contain a dashed link. The arrows indicate such products originating from the states with $(m_1, m_2) = (\frac{9}{2}, \frac{3}{2})$ and $(\frac{9}{2}, -\frac{5}{2})$, respectively

matrix, this representation is very lucid: edges arise only along the diagonals between neighbouring points. This feature is the second ingredient necessary for the occurrence of quasi-degeneracies. Now, superposing the graphical representation of two correlated subspaces provides an appropriate means for comparing the perturbation matrices of those subspaces. This is illustrated in Fig. 5a and b for the subspaces (A_{1s}, A_{1a}) and (A_{1s}, B_{3s}) , where we use the following notation:

Table 5. Splitting order ν (3rd column) and number of correlated levels N_ν (4th column) for the XY-model with pure exchange anisotropy ($\alpha = 0$) around $(\alpha, \gamma) = (0, 1)$, indicated for the subspace pairs of classes M_1 , M_6 and M_7

M_i	(I, I')	ν	N_ν
M_1	$(A_{1s}, A_{1a}) (B_{1s}, B_{1a})$ $(B_{2s}, B_{2a}) (B_{3s}, B_{3a})$	$m_1 - m_2 $	$s + \frac{1}{2} - \nu$
M_6	$(A_{1s}, B_{3s}) (A_{1a}, B_{3a})$ (B_{1s}, B_{2s}) (B_{1a}, B_{2a})	$m_1 + m_2$	$s + \frac{1}{2} - \frac{1}{2}\nu$ $s + 1 - \frac{1}{2}\nu$ $s - \frac{1}{2}\nu$
M_7	(A_{1s}, B_{3a}) (A_{1a}, B_{3s}) $(B_{1s}, B_{2s}) (B_{1a}, B_{2a})$	$m_1 - m_2$	$s - \frac{1}{2}\nu$ $s + 1 - \frac{1}{2}\nu$ $s + \frac{1}{2} - \frac{1}{2}\nu$

- A correlated pair of states $|n, I\rangle$ and $|n, I'\rangle$ is represented by a full circle.
- An uncorrelated state is represented by an open circle.
- A pair $(V_{nn'}^I, V_{nn'}^{I'})$ of identical matrix elements is represented by a full line linking the corresponding full circles.
- Non-identical perturbation-matrix elements are represented by dashed lines.

In analogy to Feynman graphs, the cyclic products $V_{nk_1} \cdots V_{k_{\nu-1}n}$ arising in the ν th order contribution of the perturbation series (14) show up as closed paths of length ν in this graphical representation of V (Fig. 5).

Notice that non-equivalent matrix elements do not exist *inside* the triangle defined by $|m_2| < m_1 - 2$ (cf. Appendix 5). They only arise in two cases:

- as non-diagonal elements to an uncorrelated state if $|m_2| = m_1$, and
- as diagonal elements if $|m_2| = m_1 - 1$.

The order $\nu_n^{(I, I')}$ of the level splitting of a pair $(|n, I\rangle, |n, I'\rangle)$ of correlated states is determined by the length of the shortest cyclic product which is not identical in both subspaces. This length can be read off from the graphical representation in Fig. 5 as the length of the shortest closed path containing non-equivalent (dashed) lines. In this figure the paths are indicated for two examples with $n = (\frac{9}{2}, \frac{3}{2})$ and $n = (\frac{9}{2}, -\frac{5}{2})$. Their respective lengths are $\nu_n(A_{1s}, A_{1a}) = 3$ and 2 in Fig. 5a, and $\nu_n(A_{1s}, B_{3s}) = 6$ and 2 in Fig. 5b. The general expressions for $\nu_n^{(I, I')}$, which follow immediately from this graphical representation, are displayed in the 4th column of Table 5.

We emphasize that the level splitting of quasi-degenerate levels depends algebraically on λ with integer exponents. Log-log plots of the λ -dependence of the level splitting, displayed in Fig. 6a and b for spins of length $s = 9/2$, illustrate this result for the subspace combinations (A_{1s}, A_{1a}) and (A_{1s}, B_{3s}) , respectively. This power-law behaviour is characteristic for tunneling in spin systems [7, 8]. The number N_ν of quasi-degenerate levels which split with a given exponent ν can be deduced from the graphical representation by counting the number of non-equivalent shortest paths of length ν . Note that the total number of correlated levels $\sum_\nu N_\nu$ equals the dimension $d_1 = (2s+1)(2s-1)/8$ of the smaller subspace. Depending on the subspace combination,

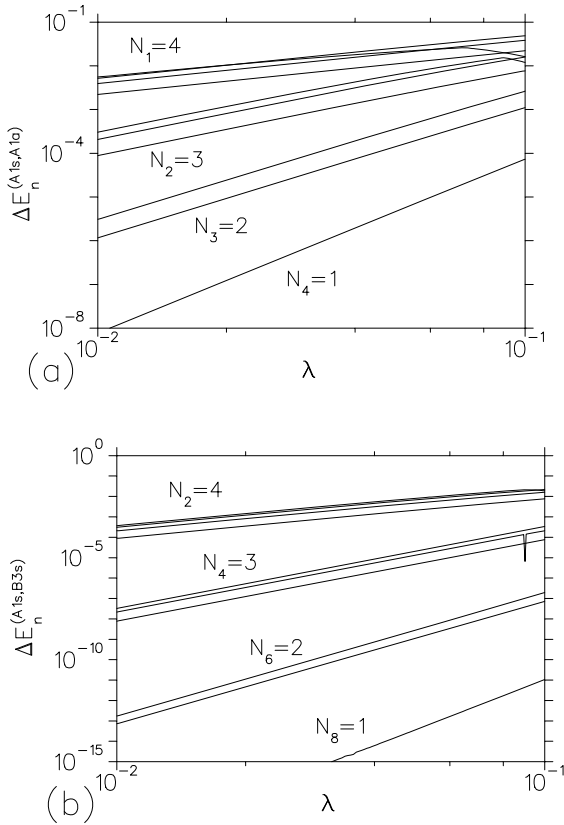


Fig. 6a,b. Double-logarithmic plot of nearest level spacings $\Delta E_n^{(I,I')}$ for $\alpha = 0$ in the vicinity of $\gamma = 1$ ($\lambda = (1 - \gamma)/(1 + \gamma)$) for spin length $s = 9/2$ (10 level pairs): **a** $(I, I') = (A_{1s}, A_{1a})$ **b** $(I, I') = (A_{1s}, B_{3s})$. All levels are degenerate for $\lambda = 0$. The lines are well described by $\log \Delta E_n^{(I,I')} \approx \nu \log \lambda + \text{const.}$, where the slope ν is the splitting order. The number of level pairs N_ν with splitting order ν is in agreement with the theoretical results (cf. Table 5)

the maximum order assumes the value $s - 1/2$ or $2s$. For the case of spin length $121/2$ displayed in Fig. 1a and b, this corresponds to a splitting proportional to λ^{60} and λ^{121} , respectively. It is obvious that for not too large values of λ such a splitting can no longer be resolved numerically.

The prefactor η_n in (19) can be calculated explicitly for all correlated pairs, but we only give the result for the ground levels. The ground states of the unperturbed system (10) are $|s, s\rangle$ and $| -s, -s\rangle$ with energy $E_0 = -1$ (in units of $J\hbar^2 s^2$). Classically these states correspond to the stationary configurations of both spins pointing in the direction of the x -axis or both in the opposite direction. They transform into each other under the symmetry transformation C_2^y (or equivalently C_2^z). Accordingly, the symmetrized states $|(s, s), B_{1s}\rangle$ and $|(s, s), B_{2s}\rangle$ form a correlated pair. Their energy levels split with order $\nu_n = 2s$ in λ (cf. Table 5). Explicit evaluation of the perturbation series (19) (cf. appendix 5) yields

$$\Delta E_{(s,s)} = 8 \left(\frac{\lambda}{4} \right)^{2s} + o(\lambda^{2s}) \quad [\cdot J\hbar^2 s^2]. \quad (21)$$

A rough estimation shows that the higher-order terms can be neglected as long as $\lambda \lesssim 2/\sqrt{s}$.

With the perturbational considerations, which were exposed in this section, one can also understand the aligned arrangement of the dots in the $(E_n, \Delta E_n)$ -plots (Figs. 1 and 2). The lines of dots are directly related to the order ν_n of the level splitting. Each line is characterized by a constant value of ν_n , the dots of the lines corresponding to the different correlated states occurring for this particular ν_n . The lines arise because the prefactor in (19) depends smoothly on the energy. In the semi-classical limit, the dots merge to continuous lines.

5. Summary and discussion

In the preceding sections we have investigated the quasi-degeneracies of energy levels in the quantum XY-model. Most quasi-degeneracies found on the $\alpha = 0$ axis in the parameter plane are related to exact degeneracies for $\gamma = -1, 0$, or 1 .

It has been shown explicitly how to evaluate, by means of degenerate perturbation theory, the level splitting caused by breaking the additional symmetry at $\gamma = 1$. This calculation reveals the reason for the quasi-degeneracy: most levels split in a very high order ν of the perturbation parameter γ by $\lambda = (\gamma - 1)/(\gamma + 1)$. For the ground state, ν takes its maximum value $2s$.

The exponential decrease of the level splitting with increasing spin length already suggests that the quasi-degeneracies can be interpreted as tunnel splitting. This view is highly supported by the form of the ground state and the first excited state, which, as usual in systems with tunneling, are obtained from the symmetry-related localized states $|ss\rangle$ and $| -s -s\rangle$ by symmetrisation and antisymmetrisation. Similar phenomena have been observed in a circular quantum billiard with a circular obstacle placed out of center [20]. In that case, the excentricity of the obstacle is the perturbation parameter. Tunneling between states corresponding to clockwise and counterclockwise rotating trajectories occurs because classical chaos enables transitions between these states for non-vanishing perturbation parameter.

However, certain quasi-degenerate states in the classes M_3, M_5 and M_6 , which appear near the $\gamma = 0$ axis, could not be related to exact degeneracies. (In the $(E_n^I, \Delta E_n^{(I,I')})$ plots they appear as cup-shaped structures, as on the left side of Fig. 2.) It is expected that these quasi-degeneracies are related to degeneracies somewhere else in the parameter space, but this could not be confirmed.

The absence of low-order terms in the perturbation series of the level splitting is due to the sparse matrix structure of the perturbative Hamiltonian \hat{V} . While for a system consisting of two spins of length s , the total number of matrix elements grows as s^4 , the number of non-zero matrix elements of \hat{V} grows as s^2 and the number of non-identical elements of two symmetry related perturbative Hamiltonians \hat{V}^I and $\hat{V}^{I'}$ is only proportional to s (cf. Sect. 4). The generalization of the calculation presented in Sect. 4 is straightforward for n -spin systems with 2-spin exchange interactions. Also in such systems, the perturbation matrices are typically sparse matrices, which are particularly simple if the spin-spin interaction is restricted to nearest neighbours. For a system composed of n spins, the energy eigenstates may be represented

Table 6. Coefficients for the matrix elements of the perturbation matrix $\hat{V} = -J\hat{S}_1^x\hat{S}_2^x$. The constants A, B, C, D and E refer to (A1). The constants A_0, B_0, C_0 and D_0 are defined by (A2)

Condition	A	B	C	D	E
$ m_2 < m_1 + 2$	A_0	B_0	C_0	D_0	0
$m_2 = m_1 - 2$	A_0	B_0	$\frac{1+\sigma_2}{\sqrt{2}}C_0$	D_0	0
$m_2 = -m_1 + 2$	A_0	B_0	C_0	$\frac{1+\sigma_1\sigma_2}{\sqrt{2}}D_0$	0
$m_2 = m_1 - 1$	A_0	B_0	0	D_0	$\sigma_2 C_0$
$m_2 = -m_1 + 1$	A_0	B_0	C_0	0	$\sigma_1\sigma_2 D_0$
$m_2 = m_1$	$\frac{1+\sigma_2}{2}A_0$	$\frac{1+\sigma_2}{\sqrt{2}}B_0$	0	$\frac{1+\sigma_2}{2}D_0$	0
$m_2 = -m_1$	$\frac{1+\sigma_1\sigma_2}{\sqrt{2}}A_0$	$\frac{1+\sigma_1\sigma_2}{2}B_0$	$\frac{1+\sigma_1\sigma_2}{2}C_0$	0	0
$m_2 = m_1 = \frac{1}{2}$	$\frac{1+\sigma_2}{2}A_0$	$\frac{1+\sigma_2}{\sqrt{2}}B_0$	0	0	$\frac{\sigma_1+\sigma_2}{2}D_0$
$m_2 = -m_1 = -\frac{1}{2}$	$\frac{1+\sigma_1\sigma_2}{\sqrt{2}}A_0$	$\frac{1+\sigma_1\sigma_2}{2}B_0$	0	0	$\frac{\sigma_1+\sigma_2}{2}C_0$

as points on an n -dimensional lattice (which represents a system of n ‘‘good’’ quantum numbers), and the matrix elements of the unperturbed Hamiltonian are represented as links between neighbouring lattice points. Non-identical matrix elements of symmetry-related perturbative Hamiltonians are expected to arise only at the border of this n -dimensional simplex. Consequently, we also expect quasi-degeneracies in the energy spectrum, which split in extremely high order with an external control parameter. Although the combinatorial problem is more difficult than for the case of two spins, we expect at least the calculation of the ground-state splitting to be feasible. The possibility of applying perturbation theory to calculate these high-order level splittings is a nice feature, which opens the possibility of a perturbational approach to spin tunneling. This appears to us of considerable interest in view of possible applications to macroscopic systems mentioned in the introduction.

We gratefully acknowledge discussions with R. Schilling and S. Weigert. We are also grateful to the referee calling our attention to the recent review on the WKB approach to spin tunneling by van Hemmen and Sütö [10]. A part of the numerical calculations was carried out at the CSCS in Manno/TI. This work was supported by the Swiss National Science Foundation.

Appendix A: the matrix elements of the perturbative matrix

Using the relation $\hat{S}^\pm = \hat{S}^y \pm i\hat{S}^z$ (remember that the states $|s m\rangle$ are eigenstates of \hat{S}^x !), and noting that $\hat{S}^\pm |s m\rangle = \hbar L(\pm m) |s m \pm 1\rangle$ with $L(m) = \sqrt{(s-m)(s+m+1)}$, one can write for the perturbation matrix $\hat{V} = -J\hat{S}_1^y\hat{S}_2^y$ of (11):

$$\begin{aligned} & \langle m'_1 m'_2 \sigma_1 \sigma_2 | \hat{V} | m_1 m_2 \sigma_1 \sigma_2 \rangle = \\ & = A \delta_{m'_1, m_1+1} \delta_{m'_2, m_2+1} + B \delta_{m'_1, m_1+1} \delta_{m'_2, m_2-1} \\ & + C \delta_{m'_1, m_1-1} \delta_{m'_2, m_2+1} + D \delta_{m'_1, m_1-1} \delta_{m'_2, m_2-1} \\ & + E \delta_{m'_1, m_1} \delta_{m'_2, m_2} \end{aligned} \quad (\text{A1})$$

The coefficients A, B, C, D and E depend on m_1, m_2, σ_1 and σ_2 . They are listed in Table 6 referring to some constants A_0, B_0, C_0 and D_0 which are defined in units of $J\hbar^2$ as

$$\begin{aligned} A_0 &= -\frac{1}{4}L(m_1)L(m_2), & B_0 &= -\frac{1}{4}L(m_1)L(-m_2), \\ C_0 &= -\frac{1}{4}L(-m_1)L(m_2), & D_0 &= -\frac{1}{4}L(-m_1)L(-m_2). \end{aligned} \quad (\text{A2})$$

Appendix B: calculation of the splitting amplitude of the ground levels

As exposed in Sect. 4, (19) the splitting amplitude η_n is obtained from the smallest closed loop of transition amplitudes $V_{nk_1} \dots V_{k_l n}$ differing in both subspaces. For the ground levels $E_{(s,s)}^{B_{1s}}$ and $E_{(s,s)}^{B_{2s}}$ this is the loop on the diagonal $m_1 = m_2$, with the only difference that an opposite sign appears for the diagonal element for the state $(m_1, m_2) = (\frac{1}{2}, \frac{1}{2})$. With the abbreviations $V_{m'm}^I = \langle (m', m'), I | \hat{V} | (m, m), I \rangle$ and $E_m = E_{(m,m)}(0) = -J\hbar^2 m^2$ one gets

$$\begin{aligned} \eta_{(s,s)} &= \left(V_{\frac{1}{2}, \frac{1}{2}}^{B_{1s}} - V_{\frac{1}{2}, \frac{1}{2}}^{B_{2s}} \right) \prod_{m=\frac{1}{2}}^{s-1} \frac{|V_{m+1, m}|^2}{(E_s - E_m)^2} \\ &= \frac{J\hbar^2}{2} L\left(-\frac{1}{2}\right)^2 \prod_{m=\frac{1}{2}}^{s-1} \frac{(\frac{1}{4}L(m)^2)^2}{(s+m)^2(s-m)^2} \\ &= 8 \left(\frac{1}{4}\right)^{2s} [\cdot J\hbar^2 s^2]. \end{aligned}$$

References

1. A. O. Caldeira and K. Furuya: Quantum nucleation of magnetic bubbles in a two-dimensional anisotropic Heisenberg model, *J. Phys.* **C21**, (1988), 1227–1241.
2. E. M. Chudnovsky and L. Gunther: Quantum theory of nucleation, *Phys. Rev.* **B37**, (1988), 9455–9459.
3. B. Barbara and E. M. Chudnovsky: Macroscopic quantum tunneling in antiferromagnets, *Phys. Lett.* **A145**, (1990), 205–208.
4. P. C. E. Stamp: Quantum dynamics and tunneling of domain walls in ferromagnetic insulators, *Phys. Rev. Lett.* **66**, (1991), 2802–2805.
5. A. De Franco, I. Klik, L. Gunther, A. G. Swanson, and J. S. Brooks: Macroscopic quantum tunneling in single domain magnetic particles, *J. Appl. Phys.* **63**, (1988), 4234–4236.
6. I. V. Krive and O. B. Zaslavskii: Macroscopic quantum tunneling in antiferromagnets, *J. Phys.: Condens. Matter* **2**, (1990), 9457–62.
7. M. Enz, R. Schilling: Spin tunneling in the semiclassical limit, *J. Phys.* **C19**, (1986), 1765–1770; M. Enz, R. Schilling: Magnetic field dependence of the tunneling splitting of quantum spins, *J. Phys.* **C19**, (1986), L711–L715;
8. J. L. van Hemmen and A. Sütö: Tunneling of quantum spins, *Europhys. Lett.* **1**, (1986), 481–490; *Physica* **141B**, (1986), 37–75.
9. R. Schilling: Quantum spin tunneling: A path-integral approach. In: *Quantum tunneling of magnetization*, edited by B. Barbara and L. Gunther (Kluwer, Dordrecht, 1995), 59–76.

10. J. L. van Hemmen and A. Sütö: Theory of mesoscopic quantum tunneling in magnetism: a WKB approach. In: *Quantum tunneling of magnetization*, edited by B. Barbara and L. Gunther (Kluwer, Dordrecht, 1995), 19–57.
11. L. D. Landau and E. M. Lifshitz: Quantum Mechanics. Pergamon Press, Oxford, 1965. Chapter 7.
12. D. A. Garanin: Spin tunneling: A perturbative approach. *J. Phys.* **A24**, (1991), L61–L62.
13. S. Weigert: Topologically quenched tunnel splitting in a spin system obtained from quantum-mechanical perturbation theory. *Europhys. Lett.* **26**(8), (1994), 561–564.
14. E. Magyari, H. Thomas, R. Weber, C. Kaufmann, G. Müller: Integrable and nonintegrable classical spin clusters: *Z. Phys.* **B 65**, (1987), 363–374
15. R. O. Weber: *Untersuchungen an klassischen Spinsystemen*, PhD thesis, University of Basel (1988)
16. N. Srivastava, C. Kaufmann, G. Müller: Chaos in Spin Clusters: Correlation Functions and Spectral Properties, *J. Appl. Phys.* **63** (1988), 4154
17. N. Srivastava, C. Kaufmann, G. Müller: Chaos in Spin Clusters: Quantum Invariants and Level Statistics, *J. Appl. Phys.* **67** (1990), 5627–5629
18. J. J. Sakurai: *Modern Quantum Mechanics*. Addison-Wesley (1985)
19. B. Eckhardt: Quantum mechanics in classically non-integrable systems, *Phys. Rep.* **163**, no. 4, (1988), 205–297
20. O. Bohigas, D. Boosé, R. Egdio de Carvalho and V. Marvulle: Quantum tunneling and chaotic dynamics, *Nucl. Phys.* **A 560**, (1993), 197–210.